

Localization, Decomposition, and Dictionary Learning of Piecewise-Constant Signals on Graphs

Siheng Chen, *Student Member, IEEE*, Yaoqing Yang, *Student Member, IEEE*, José M. F. Moura, *Fellow, IEEE*, Jelena Kovačević, *Fellow, IEEE*

Abstract—Motivated by the need to extract meaning from large amounts of complex data that can be best modeled by graphs, we consider three critical problems on graphs: localization, decomposition, and dictionary learning of piecewise-constant signals. These graph-based problems are related to many real-world applications, such as localizing virus attacks in cyber-physical systems, localizing stimulus in brain connectivity networks, and mining traffic events in city street networks, where the key issue is to separate localized activated patterns and background noise; in other words, we aim to find the supports of localized activated patterns. Counterparts of these problems in classical signal/image processing, such as impulse detection, foreground detection, and wavelet construction, have been intensely studied over the past few decades. We use piecewise-constant graph signals to model localized patterns, where each piece indicates a localized pattern that exhibits homogeneous internal behavior and the number of pieces indicates the number of localized patterns. For such signals, we show that decomposition and dictionary learning are natural extensions of localization, the goal of which is not only to efficiently approximate graph signals, but also to accurately find supports of localized patterns. For each of the three problems, i.e., localization, decomposition, and dictionary learning, we propose a specific graph signal model, an optimization problem, and a computationally efficient solver. The proposed solvers directly find the supports of arbitrary localized activated patterns without tuning any thresholds, which is a notorious challenge in many localization problems. We then conduct an extensive empirical study to validate the proposed methods on both simulated and real data including the analysis of a large volume of spatio-temporal Manhattan urban data. From taxi-pickup activities and using our methods, we are able to detect both everyday as well as special events and distinguish weekdays from weekends. Our findings validate the effectiveness of the approach and suggest that graph signal processing tools may aid in urban planning and traffic forecasting.

Index Terms—Signal processing on graphs, signal localization, signal decomposition, dictionary learning

I. INTRODUCTION

Today's data is being generated at an unprecedented level from a diversity of sources, including social networks, biological studies and physical infrastructure. The necessity of analyzing such complex data has led to the birth of *signal processing on graphs* [1], [2], [3], which generalizes classical signal processing tools to data supported on graphs; the data is the graph signal indexed by the nodes of the underlying graph. Recent additions to the toolbox include sampling of graph

S. Chen, Y. Yang, J. M. F. Moura and J. Kovačević are with the Dept. of Electrical and Computer Engineering. Moura and Kovačević are also with the Dept. of Biomedical Engineering (by courtesy), Carnegie Mellon University, Pittsburgh, PA, 15213 USA. Emails: {sihengc,yaoqingy,moura,jelenak}@andrew.cmu.edu.

The authors gratefully acknowledge support from the NSF through awards CCF 1421919, 1563918 and 1513936.

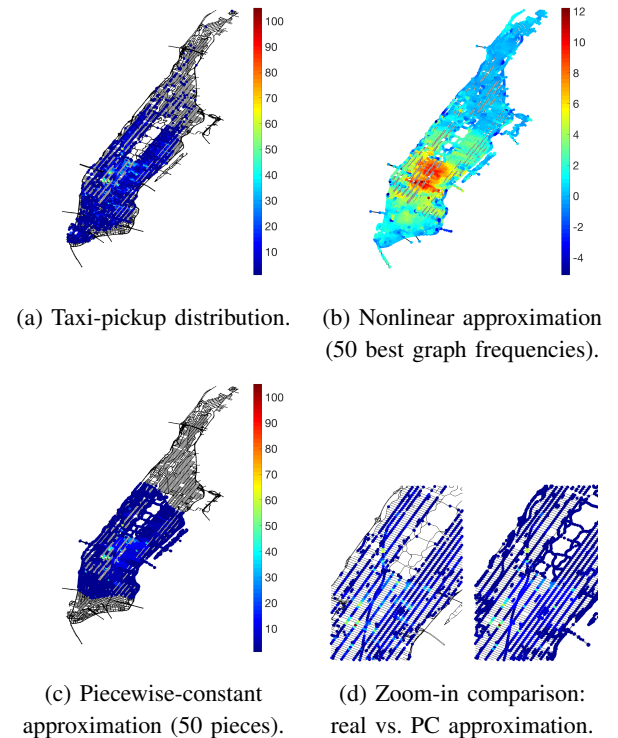


Fig. 1: Piecewise-constant approximation well represents irregular, nonsmooth graph signals by capturing the large variations on the boundary of pieces and ignoring small variations inside pieces. Plot (a) shows Taxi-pickup distribution at 7 pm on Jan 1st, 2015 in Manhattan. Visually, the distribution is well approximated by a piecewise-constant (PC) graph signal with 50 pieces in Plot (c). On the other hand, the graph frequency based approximation in Plot (b) fails to capture localized variations.

signals [4], [5], [6], [7], recovery of graph signals [8], [9], [10], [11], representations for graph signals [12], [13], [14], [15], uncertainty principles on graphs [16], [17], stationary graph signal processing [18], [19], graph-based filter banks [20], [21], [22], [23], denoising [20], [24], community detection and clustering on graphs [25], [26], [27] and graph-based transforms [28], [29], [30].

The task of finding activated signal/image supports has been intensely studied in classical signal/image processing from various aspects over the past few decades. For example, impulse detection localizes impulses in a noisy signal [31]; support recovery of sparse signals localizes sparse activations with a limited number of samples [32]; foreground detection

localizes foreground in a video sequence [33]; cell detection and segmentation localize cells in microscopy images [34] and matched filtering localizes radar signals in the presence of additive stochastic noise [35].

We consider here the counterpart problem on graphs, that is, localizing activated supports of signals in a large-scale graph, a task relevant to many real-world applications from localizing virus attacks in cyber-physical systems to activity in brain connectivity networks, to traffic events in city road networks. Similarly to classical localization problems, the key issue is to separate localized activated patterns on graphs from background noise; in other words, we aim to find the supports of localized activated patterns on graphs.

Similarly to how piecewise-constant time series are used in classical signal processing, we model localized activated patterns as piecewise-constant graph signals since they capture large variations between pieces and ignore small variations within pieces. In other words, piecewise-constant graph signals allow us to find supports of localized patterns in the graph vertex domain. Each piece in the signal indicates a localized pattern that exhibits homogeneous internal behavior while the number of pieces indicates the number of localized patterns. As an example, Figure 1 shows that a piecewise-constant graph signal can well approximate a real signal—taxi-pickup distribution in Manhattan.

While most of the work in graph signal processing happens in the graph frequency domain, we work here in the graph vertex domain because it provides better localization and is easier to visualize (Figure 1(b)). This is similar to classical image processing, where most methods for edge detection and image segmentation work in the space domain (instead of the frequency domain).

Based on the piecewise-constant graph signal model, we consider three key problems: localization, decomposition, and dictionary learning, each of which builds on the previous one. Localization identifies an activated piece in a *single* graph signal, decomposition identifies *multiple* pieces in a *single* graph signal and dictionary learning identifies *shared* activated pieces in *multiple* graph signals. The aim of studying decomposition and dictionary learning is not only for efficient approximation, but also for accurately localizing patterns.

Localization. This task is the counterpart to matched filtering in classical signal processing with the aim of identifying a set of connected nodes where the graph signal switches values—we call this an *activated piece*. For example, given a graph signal in Figure 2(a), we are looking for an underlying activated piece as in Figure 2(b). As the original signal is noisy, this task is related but not equivalent to denoising, as denoising aims to obtain a noiseless graph signal (see Figure 2(c)), which is not necessarily localized. In this paper, we focus on localizing activated pieces in noisy piecewise-constant signals when localization is, in fact, equivalent to denoising with proper thresholding.

Decomposition. This task is the counterpart to independent component analysis in classical signal processing with the aim of decomposing or representing a signal as a linear combination of building blocks—activated pieces. For example, given a graph signal in Figure 3(a), we decompose it into two activated

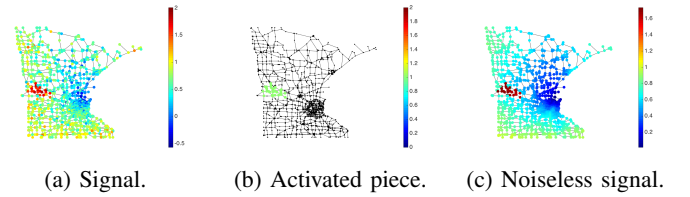


Fig. 2: Signal localization on graphs. Given a signal (a), the aim is to identify an activated piece (b) while denoising aims to obtain a noiseless signal (c). When a smooth background is ignored, localization is equivalent to denoising.

pieces, shown in (b) and (c), respectively.

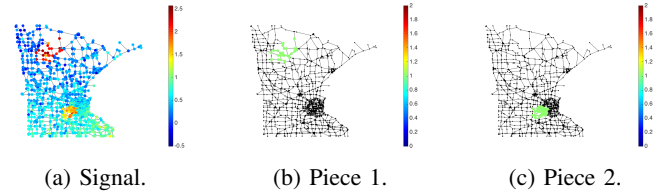


Fig. 3: Signal decomposition on graphs. Given a signal (a), we aim to decompose it into two activated pieces (b) and (c).

Dictionary learning. This task is the counterpart to sparse dictionary learning in classical signal processing with the aim of learning a graph dictionary of one-piece atoms from multiple graph signals. Instead of focusing on approximation, the proposed graph dictionary focuses on finding shared localized patterns from a large set of graph signals. For example, given the signals in Figures 4(a)–(c), we look for the underlying shared activated pieces as in Figures 4(d) and (e). This is relevant in many real-world applications that try to localize common patterns in a large data volume. For example, on weekday evenings, the area near Penn Station in Manhattan is notoriously crowded. We can model the number of passing vehicles at all the intersections by a graph signal on the Manhattan street network and use dictionary learning techniques to analyze traffic activities at various moments and automatically localize the patterns.

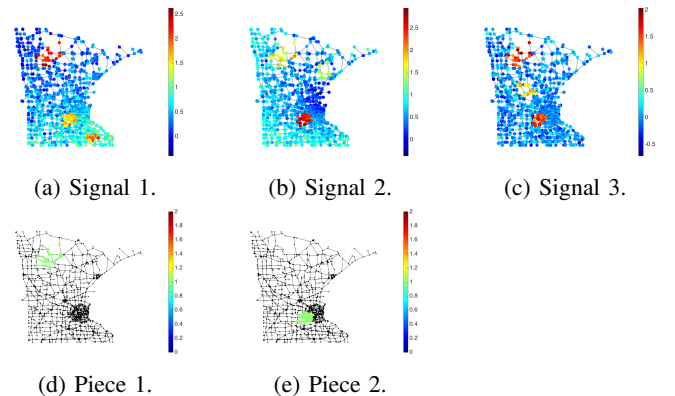


Fig. 4: Dictionary learning on graphs. Given signals (a)–(c), dictionary learning aims to find shared activated pieces (d), (e).

Related Work. We now briefly review related work on localization, decomposition and dictionary learning.

a) Localization: Signal localization has been considered from many aspects. From a signal processing perspective, people studied signal/noise discrimination [36], matched filtering [35], and support recovery of sparse signals [32]; from an image processing perspective, people studied object detection in natural and biomedical images [37], and foreground detection in a video sequence [33]; and from a data mining perspective, people studied anomaly detection [38]. Within the context of graphs, much of the literature considers detecting smooth or piecewise-constant graph signals from signals corrupted by Gaussian noise [39], [40], [41], [42]. A recent work [43] considers detecting localized graph signals corrupted by Bernoulli noise. In this paper, we localize activated pieces on graphs.

b) Decomposition: Signal decomposition/representation is at the heart of most signal processing tasks [44] as signals are represented or approximated as a linear combination of basic building blocks. Fourier analysis can be seen as spectral decomposition of signals into sinusoidal components and is widely used in communication systems. Wavelet and multiresolution techniques decompose signals into components at different scales and are widely used in image, video compression, and elsewhere [45]. Other approaches include independent component analysis [46], which aims to adaptively decompose a signal into independent components. Within the context of graphs, counterparts to classical transforms include the graph Fourier transform [1], [3], the windowed graph Fourier transform [47], and the wavelet transform [28]. In a number of works, representations are considered based on the graph Fourier domain [1], [48], [20], designing graph filters in the graph Fourier domain, and achieving representations that are localized in the graph Fourier domain. Yet others consider representations based on the vertex domain [49], [50], [41], [15], decomposing a graph into multiple sub-graphs of various sizes and achieving representations that are particularly localized in the graph vertex domain. In this paper, we look at representations based on the graph vertex domain in a data-adaptive fashion in contrast to some of the previous work where representations are designed based on the graph structure only.

c) Dictionary learning: Dictionary learning finds a sparse representation of the input data as a linear combination of basic building blocks. This task is widely studied in image processing, computer vision, and machine learning. Popular algorithms include the method of optimal directions [51], K-SVD [52] and online dictionary learning [53]. Within the context of graphs, [13] considers learning a concatenation of subdictionaries, with each subdictionary being a polynomial of the graph Laplacian matrix. This method captures the localized patterns that are limited to the exact K -hop neighbors, which is not flexible enough to capture arbitrarily shaped localized patterns. Furthermore, to update the graph dictionary, quadratic programming with a few hard constraints is needed, which is not easily scalable. We here aim to learn a graph dictionary that captures localized patterns with arbitrary shapes (not restricted to K -hop neighbors). Moreover, the learning process is scalable.

Contributions. We start with a basic localization problem whose goal is to localize an activated piece with unit magnitude in a noisy one-piece graph signal. We propose an efficient and effective solver and extend it to arbitrary magnitude. This solver is able to efficiently search for a localized pattern with arbitrary shape and directly finds supports of localized patterns without tuning a threshold, which is a notoriously challenging issue in many localization problems. Building on localization, we next consider signal decomposition and dictionary learning on graphs. We conduct extensive experiments to validate the proposed methods. The results show that cut-based localization is good at localizing the ball-shaped class and path-based localization is good at localizing the elongated class. We further apply our algorithms to analyze urban data, where our methods automatically detect events and explore mobility patterns across the city from a large volume of spatio-temporal data.

The main contributions of the paper are:

- A novel and efficient solver for graph signal localization without tuning parameters.
- A novel and efficient solver for graph signal decomposition.
- A novel and efficient solver for graph dictionary learning.
- Extensive validation of the proposed solvers on both simulated as well as real data (Minnesota road and Manhattan street networks).

Notation. Consider an undirected graph $G = (\mathcal{V}, \mathcal{E})$, where $\mathcal{V} = \{v_1, \dots, v_N\}$ is the set of nodes and $\mathcal{E} = \{e_1, \dots, e_M\}$ is the set of edges. A *graph signal* \mathbf{x} maps the graph nodes v_n to the signal coefficients $x_n \in \mathbb{R}$; in vector form, $\mathbf{x} = [x_1 \ x_2 \ \dots \ x_N]^T \in \mathbb{R}^N$. Let $C \subseteq \mathcal{V}$ be a subset of nodes; we represent it by the indicator vector,

$$\mathbf{1}_C = \begin{cases} 1, & v_i \in C; \\ 0, & \text{otherwise.} \end{cases} \quad (1)$$

that is, $\mathbf{1}_C$ is a graph signal with 1s in C and 0s in the complement node set $\bar{C} = \mathcal{V} \setminus C$. We say that the node set C is *activated*. When the node set C forms a connected subgraph, we call $C \in \mathcal{C}$ a *piece*, \mathcal{C} is the set of all pieces and $\mathbf{1}_C$ a *one-piece graph signal*.

Define a *piecewise-constant graph signal* as

$$\mathbf{x} = \sum_{i=1}^K \mu_i \mathbf{1}_{C_i},$$

with C_i a piece, μ_i a constant and K the number of pieces.

Outline of the paper. We present the three problems, graph signal localization, decomposition, and dictionary learning in Sections II, III, and IV, respectively. Section V concludes the paper and provides pointers to future research directions.

II. SIGNAL LOCALIZATION ON GRAPHS

In this section, we propose a solver for the localization problem, validating it by simulations.

Consider localizing an activated piece $C \in \mathcal{C}$ in a noisy, piecewise-constant graph signal

$$\mathbf{x} = \mu \mathbf{1}_C + \epsilon, \quad (2)$$

where $\mathbf{1}_C$ is the indicator function (1), μ is the signal strength and $\epsilon \sim \mathcal{N}(0, \sigma^2 \mathbf{I}_N)$ is Gaussian noise. We consider two cases: μ arbitrary and $\mu = 1$.

Previously, this has been formulated as a detection problem via a scan statistic searching for a most probable anomaly set. While this is similar to localizing an activated piece, it is either computationally inefficient or hindered by strong assumptions. For example, in [39], the authors analyze the theoretical performance of detecting paths, blobs and spatial temporal sets by exhaustive search, resulting in a costly algorithm, while in [42], [43], the authors aim to detect a node set with a specific cut number, resulting in a computationally efficient algorithm, but limited by strong assumptions.

We aim to efficiently localize an activated piece with arbitrary shape. The maximum likelihood estimator of the one-piece-localization problem under Gaussian noise is

$$\min_{\mu, C} \|\mathbf{x} - \mu \mathbf{1}_C\|_2^2, \quad \text{subject to } C \in \mathcal{C}. \quad (3)$$

A. Methodology

1) *Localization with unit magnitude:* Consider first (2) with a unit-magnitude signal, that is, $\mu = 1$. Then (3) reduces to

$$\min_C \|\mathbf{x} - \mathbf{1}_C\|_2^2, \quad \text{subject to } C \in \mathcal{C}. \quad (4)$$

This optimization problem is at the core of this paper. In what follows, we first look at hard thresholding as a baseline and then propose two efficient solvers for two typical and complementary classes: a ball-shaped class and an elongated class. A ball-shaped class consists of activated pieces, forming subgraphs with relatively small diameters compared to its cardinality and dense internal connections; as an opposite to a ball-shaped class, an elongated class consists of activated pieces, forming subgraphs with relatively large diameters compared to its cardinality and sparse internal connections. An extreme case of an elongated piece is a path, which is a tree with two nodes degree 1 and the other nodes degree 2. We then combine both solvers to obtain a general solver for (4).

Hard thresholding based localization. The difficulty in solving (4) comes from the constraint, which forces the activated nodes to form a connected subgraph (piece). Since we do not restrict the size and shape of a piece, searching over all pieces to find the global optimum is an NP-complete problem. We consider a simple algorithm that solves (4) in two steps: we first optimize the objective function and then project the solution onto the feasible set in (4). While this simple algorithm guarantees a solution, it is not necessarily optimal. The objective function can be formulated as

$$\min_C \|\mathbf{x} - \mathbf{1}_C\|_2^2 = \min_{\mathbf{t} \in \{0,1\}^N} \|\mathbf{x} - \mathbf{t}\|_2^2 = \min_{t_i \in \{0,1\}} \sum_{i=1}^N (x_i - t_i)^2,$$

where $\mathbf{t} \in R^N$ is a vector representation of a node set C . Since t_i are independent, we can optimize each individual element to obtain $t_i^* = 1$, when $x_i > 1/2$; and 0, otherwise. In other words, the optimum of the objective function is

$$\{v_i \in \mathcal{V} \mid x_i > \frac{1}{2}\} = \min_C \|\mathbf{x} - \mathbf{1}_C\|_2^2.$$

This step is nothing but global hard thresholding. We then project this solution onto the feasible set; that is, we solve

$$\begin{aligned} C_{\text{thr}}^* &= P_C(\arg \min_C \|\mathbf{x} - \mathbf{1}_C\|_2^2) \\ &= P_C(\{v_i \in \mathcal{V} \mid x_i > \frac{1}{2}\}), \end{aligned} \quad (5)$$

where the projection operator $P_C(C)$ extracts the largest connected component (piece) in a node set C . Thus, this solver simply performs hard thresholding and then finds a connected component among the nodes with nonzero elements on it.

Cut-based localization for ball-shaped class. The key idea in (5) is to partition nodes into activated and inactivated nodes. This is similar to graph cuts: cutting a series of edges with minimum cost and obtaining two isolated components. A small cut cost indicates that internal connection is stronger than external connection. The difference between graph cuts and our task is that graph cuts optimize edge weights, while (4) optimizes graph signal coefficients. We can adaptively update the edge weights by using graph signal coefficients and solve (4) by using efficient graph-cut solvers. Inspired by [42], [43], we add the number of edges connecting activated and inactivated nodes to the objective function to induce a connected component. Let $\Delta \in \mathbb{R}^{M \times N}$ be the *graph incidence matrix* of G [54]. When the edge e_i connects the j th to the k th node ($j < k$), the i th row of Δ is

$$\Delta_{i,\ell} = \begin{cases} 1, & \ell = j; \\ -1, & \ell = k; \\ 0, & \text{otherwise.} \end{cases} \quad (6)$$

The signal $\Delta \mathbf{1}_C \in \mathbb{R}^M$ records the first-order differences of $\mathbf{1}_C$. The number of edges connecting C and \bar{C} is

$$\|\Delta \mathbf{1}_C\|_0 = \|\mathbf{A} \mathbf{1}_C\|_1 - \mathbf{1}_C^T \mathbf{A} \mathbf{1}_C,$$

where \mathbf{A} is the adjacency matrix, $\|\mathbf{A} \mathbf{1}_C\|_1$ is the sum of the degrees of the nodes in C and $\mathbf{1}_C^T \mathbf{A} \mathbf{1}_C$ describes the internal connections within C . When there are no edges connecting activated nodes, $\|\Delta \mathbf{1}_C\|_0 = \|\mathbf{A} \mathbf{1}_C\|_1$. When all activated nodes are well connected and form a ball-shaped piece, internal connections $\mathbf{1}_C^T \mathbf{A} \mathbf{1}_C$ is large and $\|\Delta \mathbf{1}_C\|_0 \ll \|\mathbf{A} \mathbf{1}_C\|_1$. Thus, minimizing $\|\Delta \mathbf{1}_C\|_0$ induces C to be a piece. We thus solve

$$C_\lambda = P_C(\arg \min_C \|\mathbf{x} - \mathbf{1}_C\|_2^2 + \lambda \|\Delta \mathbf{1}_C\|_0), \quad (7a)$$

$$C_{\text{cut}}^* = \arg \min_{C_\lambda} \|\mathbf{x} - \mathbf{1}_{C_\lambda}\|_2^2. \quad (7b)$$

Given λ , (7a) solves the regularized optimization problem and extracts the largest connected component, while (7b) optimizes over λ to find a solution. The hard thresholding (5) is a subcase of (7b) with $\lambda = 0$. We solve (7a) using the Boykov-Kolmogorov graph cuts algorithm [55], [56]; we call this *cut-based localization*.

To understand the regularized problem (7a) better, we have

$$\begin{aligned} &\min_C \|\mathbf{x} - \mathbf{1}_C\|_2^2 + \lambda \|\Delta \mathbf{1}_C\|_0 \\ &= \min_{\mathbf{t} \in \{0,1\}^N} \|\mathbf{x} - \mathbf{t}\|_2^2 + \lambda \|\Delta \mathbf{t}\|_0 \\ &= \min_{t_i \in \{0,1\}} \sum_i ((x_i - t_i)^2 + \lambda \sum_{j \in \text{Nei}(i)} |t_i - t_j|), \end{aligned}$$

where $\text{Nei}(i)$ is the neighborhood of the i th node. That is, we have $t_i^* = 1$ when

$$(x_i - 1)^2 + \lambda \sum_{j \in \text{Nei}(i)} |x_j - 1| < x_i^2 + \lambda \sum_{j \in \text{Nei}(i)} |x_j|.$$

The solution is

$$(t_{\text{cut}}^*)_i = \begin{cases} 1, & x_i > \frac{1}{2} + \frac{\lambda}{2}(\alpha_0 - \alpha_1); \\ 0, & \text{otherwise,} \end{cases} \quad (8)$$

with α_1, α_0 the number of neighbors of x_i with value 1 and 0, respectively. Thus, (8) is nothing but adaptive local thresholding, where the value of each element depends on the values of its neighbors. This explains why cut-based localization outperforms hard thresholding.

Path-based localization for elongated class. Cut-based localization (7a) is better suited to capturing ball-shaped pieces than elongated pieces. For example, to solve (4), we introduced $\|\Delta \mathbf{1}_C\|_0$ in (7a) to promote fewer connections between activated nodes and inactivated ones. This is because when C is a ball-shaped piece, $\mathbf{1}_C^T \mathbf{A} \mathbf{1}_C$ is large (see Figures 5(a)–(b)). An extreme case is that C is fully connected, C forms a ball-shaped piece and $\mathbf{1}_C^T \mathbf{A} \mathbf{1}_C = |C|(|C| - 1)/2$, which is large enough for graph cuts to capture.; however, when nodes in C are weakly connected, for example, when C forms a path, $\mathbf{1}_C^T \mathbf{A} \mathbf{1}_C = |C| - 1$, which is too small for graph cuts to capture.

To address elongated pieces, we consider two methods. The first method promotes elongated shape based on convex optimization. We start by restricting $\|\mathbf{A} \mathbf{1}_C\|_\infty$, the maximum degree of the nodes in the activated piece to be at most 2, promoting an elongated shape, and then solve the following optimization problem:

$$\min_C \|\mathbf{x} - \mathbf{1}_C\|_2^2, \quad \text{subject to} \quad \|\mathbf{A} \mathbf{1}_C\|_\infty \leq 2.$$

This constraint requires that each activated node connect to at most two activated nodes, which promotes elongated shape. To solve this efficiently, we relax the problem to a convex one,

$$\begin{aligned} \mathbf{t}_{p_1}^* &= \arg \min_{\mathbf{t} \in \mathbb{R}^N} \|\mathbf{x} - \mathbf{t}\|_2^2, \\ \text{subject to } \|\mathbf{A} \mathbf{t}\|_\infty &\leq 2 \quad \text{and} \quad 0 \leq \mathbf{t} \leq 1. \end{aligned}$$

We then set various thresholds for $\mathbf{t}_{p_1}^*$, extract the largest connected component and optimize over the threshold to get

$$\begin{aligned} C_\lambda &= \mathcal{P}_C(\mathbf{1}_{\mathbf{t}_{p_1}^* \geq \lambda}), \\ C_{p_1}^* &= \arg \min_{C_\lambda} \|\mathbf{x} - \mathbf{1}_{C_\lambda}\|_2^2. \end{aligned}$$

The solution promotes an elongated shape, but does not constrain it to an exact path.

The second method searches for an exact path based on the shortest-path algorithm, leading to

$$C_{p_2}^* = \arg \min_{C \text{ is a path}} \|\mathbf{x} - \mathbf{1}_C\|_2^2 + \lambda|C|, \quad (9)$$

where the regularization parameter $\lambda = 2x_{\max} - 1$ with x_{\max} the maximum element in \mathbf{x} , guaranteeing that shortest-path algorithm will work later. The optimization problem (9) can be implemented in two steps as follows:

$$\min_{\text{all pairs of } s, t} \left(\min_{C \text{ connects } s, t} \|\mathbf{x} - \mathbf{1}_C\|_2^2 + \lambda|C| \right).$$

We first fix two end points s and t and find the optimal path C connecting s and t , and then enumerate all pairs of end points and find the globally optimal path. We will show that the first step can be solved exactly by the shortest-path algorithm.

The objective function of (9) can be rewritten as

$$\begin{aligned} \|\mathbf{x} - \mathbf{1}_C\|_2^2 + \lambda|C| &= \mathbf{x}^T \mathbf{x} - 2\mathbf{1}_C^T \mathbf{x} + (1 + \lambda)\mathbf{1}_C^T \mathbf{1} \\ &= \mathbf{x}^T \mathbf{x} + 2\mathbf{1}_C^T \mathbf{y}, \end{aligned}$$

where $\mathbf{y} = \frac{1+\lambda}{2} \mathbf{1} - \mathbf{x}$. Since C is the only variable, minimizing (9) is equivalent to minimizing $\mathbf{1}_C^T \mathbf{y}$.

We consider a graph with edge weight

$$W_{i,j} = \begin{cases} \frac{y_i + y_j}{2}, & (i, j) \in \mathcal{E}; \\ \infty, & \text{otherwise.} \end{cases}$$

Let C be a path connecting two end points s and t . The path weight of C is

$$\sum_{i,j \in C} W_{i,j} = \sum_{k \in C} y_k - \frac{y_s + y_t}{2} = \mathbf{1}_C^T \mathbf{y} - \frac{y_s + y_t}{2}.$$

This indicates that given two end points s and t , minimizing $\mathbf{1}_C^T \mathbf{y}$ is equivalent to minimizing the path weight. Since $\lambda = 2x_{\max} - 1$, all edge weights are nonnegative. We can then use the shortest-path algorithm to efficiently compute the short paths between all node pairs [57] and graph coarsening techniques to reduce the number of nodes and boost the speed [58], [59].

Finally, the elongated piece is obtained by choosing the one with a smallest objective value in (4).

$$C_{\text{path}}^* = \arg \min_{C \in \{C_{p_1}^*, C_{p_2}^*\}} \|\mathbf{x} - \mathbf{1}_C\|_2^2. \quad (10)$$

We call this *path-based localization*.

Combined solvers. We combine the cut-based localization C_{cut}^* and the path-based localization C_{path}^* by choosing the one with a smaller objective value. The final solution to localize an arbitrarily shaped piece is

$$C^* = \text{Loc}_1(\mathbf{x}) = \arg \min_{C \in \{C_{\text{cut}}^*, C_{\text{path}}^*\}} \|\mathbf{x} - \mathbf{1}_C\|_2^2, \quad (11)$$

where $\text{Loc}_1(\cdot)$ is the operator that finds an activated piece with unit magnitude. This solution is not the global optimum of (4); it considers two typical and complementary subsets in the feasible set, and combines a graph-cut solver, a convex programming solver and a shortest-path solver, all of which are efficient. Note that detection or localization techniques usually need to set thresholds; however, this localization solver (11) is parameter-free and directly outputs the supports of a localized pattern. In Section II-B, we validate it empirically.

2) *Localization with unknown magnitude:* We next consider a more general case where the magnitude of the activated piece is unknown, (2), with the associated optimization problem (3).

We iteratively solve C and μ until convergence; that is, given C , we optimize over μ and then given μ , we optimize over C . In the k th iteration,

$$\begin{aligned} \mu^{(k)} &= \min_{\mu} \|\mathbf{x} - \mu \mathbf{1}_{C^{(k)}}\|_2^2 = \frac{\mathbf{x}^T \mathbf{1}_{C^{(k)}}}{\mathbf{1}_{C^{(k)}}^T \mathbf{1}_{C^{(k)}}}, \\ C^{(k)} &= \text{Loc}_1\left(\frac{1}{\mu} \mathbf{x}\right). \end{aligned}$$

We obtain a pair of local optima by alternately minimizing these two variables. We denote this solver by

$$\mu^*, C^* = \text{Loc}_{\text{unknown}}(\mathbf{x}). \quad (12)$$

B. Experimental Validation

We test our localization solver on two graphs: the Minnesota road network and the Manhattan street network. On each graph, we consider localizing two classes of simulated graph signals with different activated sizes under various noise levels.

1) *Minnesota road network*: We model this network as a graph with its 2,642 intersections as nodes and 3,342 road segments between intersections as undirected edges. We simulate ball-shaped and elongated classes of one-piece graph signals.

Ball-shaped class. We generate a ball-shaped piece by randomly choosing one node as the center node and assigning all others within $k = 5$ or $k = 10$ steps of it to an activated node set; see Figures 5(a)–(b) for examples. Green (lighter)/black (darker) nodes indicate activated/inactivated nodes, respectively. We aim to localize activated pieces from noisy one-piece graph signals with magnitude $\mu = 1$. We vary the noise variance σ^2 from 0.1 to 1 with interval 0.1 and for each randomly generate 1,000 noisy one-piece graph signals.

We measure the quality of the localization with two measures: the Hamming distance and the F_1 score. The Hamming distance emphasizes the difference between two sets while the F_1 score emphasizes their intersection; the higher the F_1 score, or the lower the Hamming distance, the better the localization quality.

The *Hamming distance* is equivalent to the Manhattan distance between two binary graph signals, that is, it counts the total number of mismatches between the two,

$$d_H(\hat{C}, C) = \|\mathbf{1}_{\hat{C}} - \mathbf{1}_C\|_1 = |C \cup \hat{C}| - |C \cap \hat{C}|,$$

where C is the ground truth for the activated piece and \hat{C} is the localized piece. The lower the Hamming distance the better the quality: it reaches its minimum value at $d_H(\hat{C}, C) = 0$.

The F_1 score is the harmonic mean of the precision and recall and measures the matching accuracy,

$$F_1(\hat{C}, C) = 2 \frac{\text{precision}(\hat{C}, C) \cdot \text{recall}(\hat{C}, C)}{\text{precision}(\hat{C}, C) + \text{recall}(\hat{C}, C)},$$

where precision is the fraction of retrieved instances that are relevant (true positives over the sum of true positives and false positives), while recall is the fraction of relevant instances that are retrieved (true positive over the sum of true positives and false negatives) [60]. Thus, with true positives = $|C \cap \hat{C}|$, sum of true positives and false positives = $|\hat{C}|$ and the sum of the true positives and false negatives = $|C|$, we have

$$F_1(\hat{C}, C) = 2 \frac{|C \cap \hat{C}|}{|C| + |\hat{C}|}.$$

The higher the F_1 score the better the quality: it reaches its maximum value at $F_1 = 1$ and minimum value at $F_1 = 0$.

Figures 5(c)–(d) show the F_1 scores and Figures 5(e)–(f) the Hamming distances of localizing ball-shaped pieces with radii $k = 5$ and 10 (left and right columns, respectively) as functions of the noise variance. Each figure compares hard thresholding (5) (hard, grey-solid line), path-based localization (10) (path, yellow-circle line), cut-based localization (7b) (cut number, purple-square line), combined localization (11) (combine, red-solid line), local-set-based piecewise-constant dictionary (LSPC, green-square line) [15], trend filtering on graphs (TF) [61] and graph Laplacian denoising (gLap) [3]. LSPC is a predesigned graph dictionary and we use the matching pursuit algorithm to choose one atom to localize an activated piece. Trend filtering on graphs and graph Laplacian

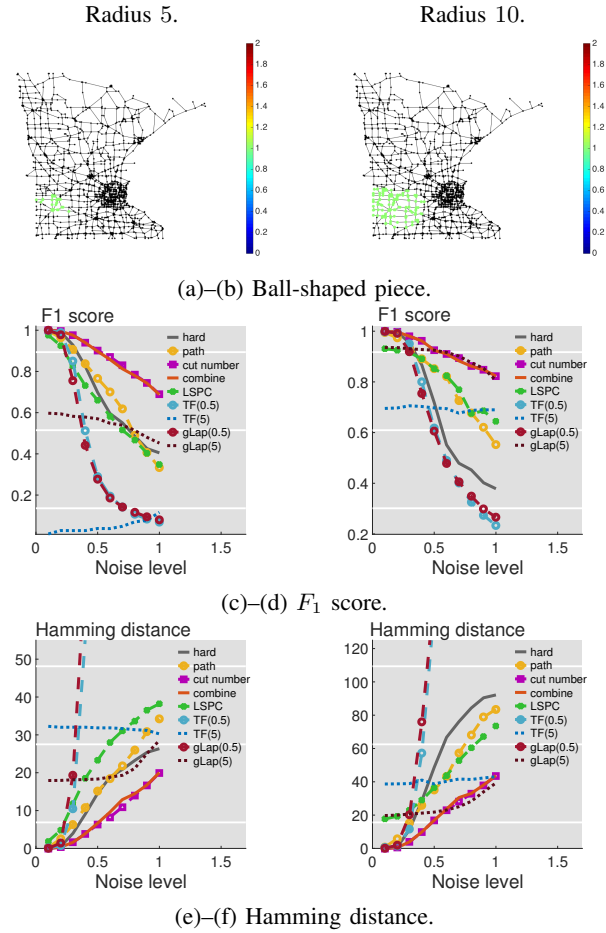


Fig. 5: Localizing ball-shaped pieces in the Minnesota road network as a function of the noise level using hard thresholding (grey-solid line), path-based localization (10) (yellow-circle line), cut-based localization (7b) (purple-square line), combined localization (11) (red-solid line), local-set-based piecewise-constant (green-square line), trending filtering on graphs ($\lambda = 0.5$ light-blue-circle line, $\lambda = 5$ dark-blue-dashed line) and graph Laplacian denoising ($\lambda = 0.5$ light-brown-circle line, $\lambda = 5$ dark-brown-dashed line). Cut-based localization provides the most robust performance.

denoising are denoising algorithms, which solve the following two optimization problems, respectively,

$$\begin{aligned} \text{TF}(\lambda) : \quad & \min_{\mathbf{t}} \|\mathbf{x} - \mathbf{t}\|_2^2 + \lambda \|\Delta \mathbf{t}\|_1, \\ \text{gLap}(\lambda) : \quad & \min_{\mathbf{t}} \|\mathbf{x} - \mathbf{t}\|_2^2 + \lambda \mathbf{t}^T \mathbf{L} \mathbf{t}, \end{aligned}$$

where λ is a tuning parameter, Δ is the graph incidence matrix (6), and \mathbf{L} is the graph Laplacian matrix. $\|\Delta \mathbf{t}\|_1$ promotes localized adaptivity and $\mathbf{t}^T \mathbf{L} \mathbf{t}$ promotes smoothness. When λ is small, both solutions are close to the noisy graph signal; when λ is large, both solutions are regularized to be either localized or smooth. We expect that a small λ works better in a noiseless case and a large λ works better in a noisy case. After obtaining the denoised solution \mathbf{t}^* , we implement hard thresholding with threshold $\mu/2 = 0.5$ to localize the activated piece. To test the sensitivity to the tuning parameter, we also

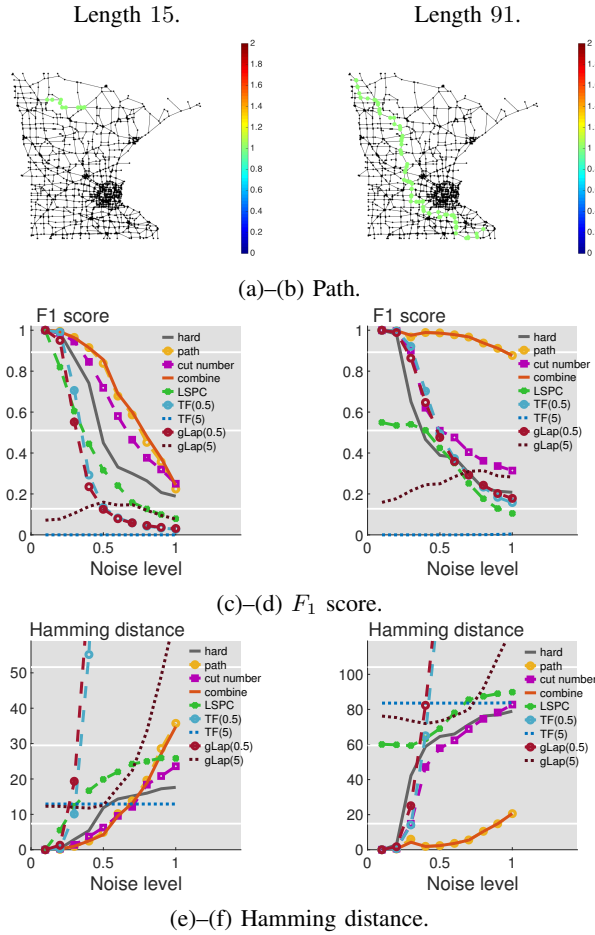


Fig. 6: Localizing paths in the Minnesota road network as a function of noise level using hard thresholding (grey-solid line), path-based localization (10) (yellow-circle line), cut-based localization (7b) (purple-square line), combined localization (11) (red-solid line), local-set-based piecewise-constant (green-square line), trending filtering on graphs ($\lambda = 0.5$ light-blue-circle line, $\lambda = 5$ dark-blue-dashed line) and graph Laplacian denoising ($\lambda = 0.5$ light-brown-circle line, $\lambda = 5$ dark-brown-dashed line). Path-based localization provides the most robust performance.

vary λ as either 0.5 or 5 in our experiments. Trend filtering on graphs and graph Laplacian denoising involve two tuning parameters: regularization parameter λ and threshold; however, neither method provides a guideline by which to choose those parameters in practice. Our proposed localization method (11), on the other hand, is parameter-free.

We observe that: (1) Cut-based localization provides the most robust performances; hard thresholding is a special case of cut-based localization, path-based localization is designed for capturing elongated pieces, LSPC is a data-independent dictionary and cannot adapt the shape of its atom to the given piece, graph Laplacian denoising with careful parameter selection works well for large activated pieces but still fails to localize small activated pieces as the smooth assumption cannot capture localized variation. Trending filtering on graphs works well in denoising of a piecewise-constant graph signal;

however, it may not work well in localization as the output is real and the threshold is hard to choose. Here the threshold is $\mu/2 = 0.5$, which sometimes works well and sometimes rules out the entire output. We also see that both graph Laplacian denoising and trending filtering on graphs are sensitive to the tuning parameter λ . The advantages of cut-based localization compared to other methods are: it is parameter-free, scalable and robust to noise. (2) Noise level influences localization performance; as it grows, the F_1 score decreases and the Hamming distance increases. (3) The size of the activated piece influences localization; localizing a piece with radius 10 is easier than localizing a piece with radius 5; this was also observed in [43].

Elongated class. We generate an elongated path by randomly choosing two nodes as starting and ending nodes and computing the shortest path between the two. We look at two classes of path lengths: between 10 to 15 and longer than 80¹; see Figures 6(a)–(b) for examples. We aim to localize activated paths with magnitude $\mu = 1$ from noisy path graph signals. We vary the noise variance σ^2 from 0.1 to 1 with interval 0.1 and for each randomly generate 1,000 noisy path graph signals. We measure the quality of the localization by the Hamming distance and F_1 score.

Figures 6(c)–(d) and (e)–(f) show the F_1 scores and the Hamming distances, respectively, of localizing elongated pieces with lengths 15 and 91 as functions of the noise variance. We compare the same methods as in Figure 5.

We observe that: (1) Path-based localization performs the best; it is also parameter-free, scalable and robust to noise. (2) When the path is short, cut-based localization and path-based localization perform similarly; when the path is long, path-based localization significantly outperforms cut-based localization. (3) Noise level influences localization performance; as it grows, the F_1 score decreases and the Hamming distance increases. (4) The path length influences localization performance. Similarly to what we observed in the ball-shaped case, it is much harder to localize a short path because a small activation provides less information.

2) *Manhattan street network:* We model this network as a graph with its 13,679 intersections as nodes and 17,163 city streets as undirected edges. We generate two classes of one-piece graph signals: a ball-shaped Central Park piece and a Fifth Avenue path. We compare results with those from the Minnesota road network to validate our conclusions.

Central Park. Figures 7(a)–(d) show a piece activating the nodes in Central Park, a noisy version with noise variance $\sigma^2 = 1$ and the activated piece provided by cut-based and path-based localization, respectively. Even when the graph signal is corrupted by a high level of noise, cut-based localization still provides accurate localization, while path-based localization fails to localize Central Park. Figures 7(e)–(f) show the F_1 score and Hamming distance when localizing Central Park as a function of the noise level, respectively. The results are averaged over 1,000 runs. Cut-based localization provides the most robust performance, which is consistent with what we observed with the Minnesota road network. Both trend filtering and graph Laplacian denoising work well at times, but are

¹The path length is the geodesic distance between the two end nodes.

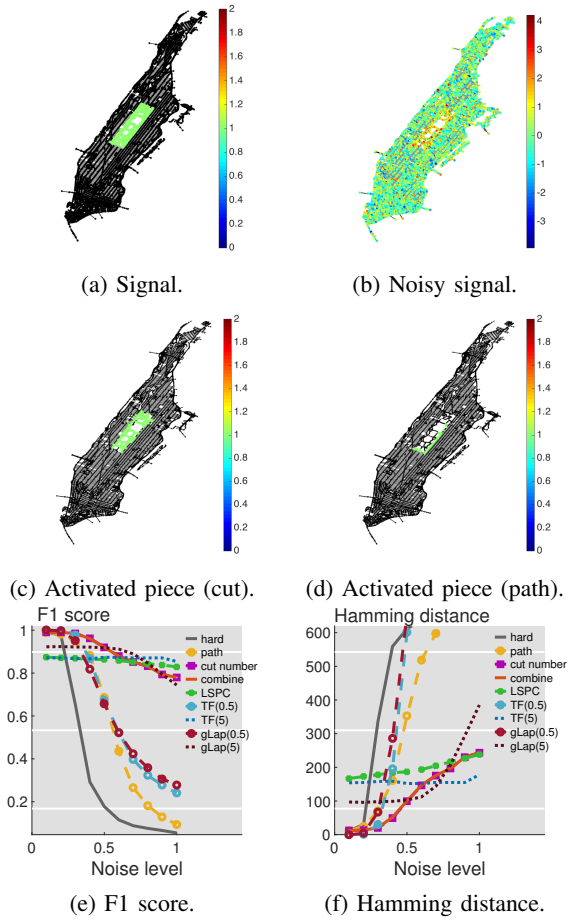


Fig. 7: Localizing (a) Central Park in the Manhattan street network as a function of the noise level from (b) its noisy version. (c) Activated piece obtained by cut-based localization with $F_1 = 0.81$ and $d_H = 214$. (d) Activated piece obtained by path-based localization with $F_1 = 0.24$ and $d_H = 586$. Cut-based localization outperforms path-based localization.

sensitive to the tuning parameter λ . Since neither method provides a guideline by which to choose the parameter, their performances may be unstable. LSPC is less sensitive to noise and slightly outperforms the other methods when the noise level is high. Since LSPC is data-independent, it chooses the most relevant predefined atom to fit a noisy signal; on the other hand, as a data-adaptive method, cut-based localization designs an atom from the noisy signal and easily fits noisy data. Overall, the localization performance of LSPC depends highly on the shape of its atoms: when LSPC has a predefined atom matching the ground truth, it is robust to noise and provides effective localization performance; when this is not the case, it fails to localize well.

Fifth Avenue. Figures 8(a)–(d) show a piece activating the nodes along Fifth Avenue, a noisy version with noise variance $\sigma^2 = 1$ and the activated piece provided by cut-based localization and the activated piece provided by path-based localization, respectively. When the graph signal is corrupted by a high level of noise, both cut-based localization and path-based localization fail to localize Fifth Avenue. Figures 8(e)–

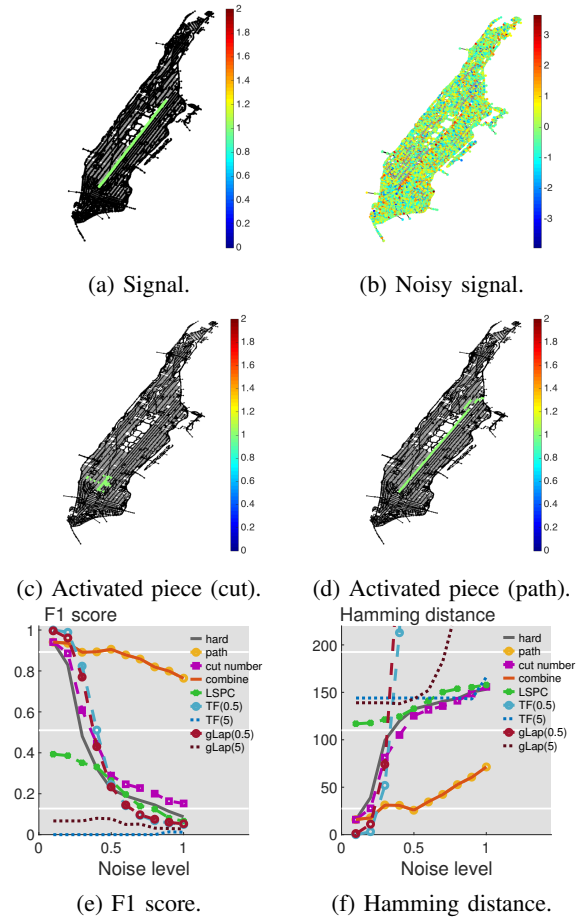


Fig. 8: Localizing (a) Fifth Avenue in the Manhattan street network as a function of the noise level from (b) its noisy version. (c) Activated piece obtained by cut-based localization with $F_1 = 0.24$ and $d_H = 144$. (d) Activated piece obtained by path-based localization with $F_1 = 0.85$ and $d_H = 43$. Path-based localization outperforms cut-based localization.

(f) show the F_1 score and Hamming distance when localizing Fifth Avenue as a function of the noise level, respectively. The results are averaged over 1,000 runs. We see that the path-based localization significantly outperforms all the other localization methods under various noise levels. This is similar to what we observed with the Minnesota road network.

III. SIGNAL DECOMPOSITION ON GRAPHS

We now extend localization discussion by considering multiple activated pieces making it a decomposition problem. We extend the the localization problem solver in Section II to the decomposition problem and validate it through simulations.

Consider localizing K activated pieces C_i , $i = 1, 2, \dots, K$, in a noisy, piecewise-constant graph signal

$$\mathbf{x} = \sum_{i=1}^K \mu_i \mathbf{1}_{C_i} + \epsilon,$$

where $\mathbf{1}_C$ is the indicator function (1), $K \ll N$, C_i are connected and $\epsilon \sim \mathcal{N}(0, \sigma^2 \mathbf{I}_N)$ is Gaussian noise.

Our goal is to develop an algorithm to efficiently decompose such a graph signal into several pieces. The corresponding optimization problem is

$$\min_{\mu_i, C_i} \left\| \mathbf{x} - \sum_{i=1}^K \mu_i \mathbf{1}_{C_i} \right\|_2^2, \quad \text{subject to } C_i \in \mathcal{C}. \quad (13)$$

When the number of activated pieces $K = 1$, the decomposition problem (13) becomes the localization problem (4). This problem is similar to independent component analysis in classical signal processing, whose goal is to decompose a signal into several independent components. Here we consider a piece in the graph vertex domain as a component and we allow the pieces to overlap for flexibility.

A. Methodology

The goal now is not only to denoise or approximate a graph signal, which would only give $\sum_{i=1}^K \mu_i \mathbf{1}_{C_i}$ but to analyze it through decomposition as well; that is, we localize each piece and estimate its corresponding magnitude, yielding μ_i and C_i . Since a graph signal is decomposed into several one-piece components, we call this *piecewise-constant decomposition*.

To solve the optimization problem (13), we update one piece at a time by coordinate descent [62]. When we freeze other variables, optimizing over μ_i and C_i is equivalent to localization with unknown magnitude in Section II-A2, because

$$\mathbf{x} - \sum_{j \neq i} \mu_j \mathbf{1}_{C_j} = \mu_i \mathbf{1}_{C_i} + \epsilon$$

is a one-piece graph signal. Thus, for each piece, we solve the localization problem (3) by using the localization solver (12),

$$\mu_i^*, C_i^* = \text{Loc}_{\text{unknown}}(\mathbf{x} - \sum_{j \neq i} \mu_j \mathbf{1}_{C_j}).$$

We iteratively update each piece until convergence to obtain a series of solutions providing a local optimum [62].

B. Experimental Validation

We validate the piecewise-constant decomposition solver on the Manhattan street network through two tasks: (1) We simulate a series of piecewise-constant graph signals by a linear combination of one-piece signals, each with a particular ZIP code; our goal is to recover ZIP codes from signal observation; (2) We decompose and analyze two real graph signals in Manhattan, restaurant distribution and taxi-pickup activity. For restaurant distribution, we extract data from the restaurant inspection results of New York City provided by Department of Health and Mental Hygiene²; for taxi-pickup activity, we use a 2015 public dataset of taxi pickups³.

1) *Signal Decomposition on Graphs: Localizing ZIP codes:* There are 43 ZIP codes in Manhattan. In each study, we randomly select two of those and generate a piecewise-constant graph signal,

$$\mathbf{x} = \mu_1 \mathbf{1}_{\text{ZIP}_1} + \mu_2 \mathbf{1}_{\text{ZIP}_2} + \epsilon,$$

where the signal strength is uniformly distributed $\mu_i \sim \mathcal{U}(0.5, 1.5)$; node set ZIP_i indicates the nodes belonging to

²Data from <https://data.cityofnewyork.us/Health/DOHMH-New-York-City-Restaurant-Inspection-Results/xx67-kt59>

³Data from http://www.nyc.gov/html/tlc/html/about/trip_record_data.shtml.

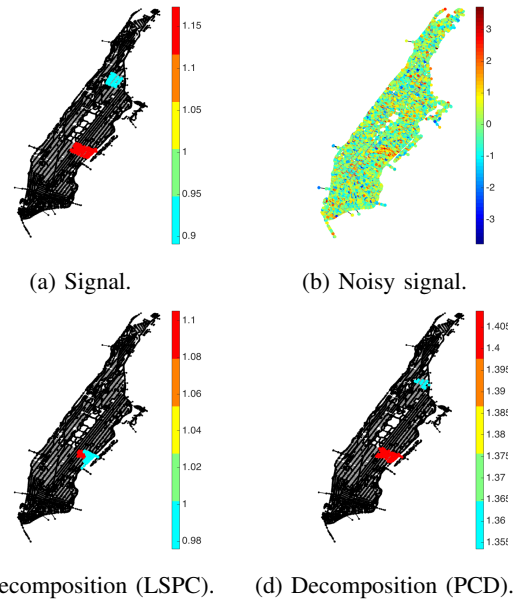


Fig. 9: Localizing a piecewise-constant graph signal associated with ZIP codes 10128 and 10030. LSPC fails to localize ZIP code 10030, but PCD successfully localizes both ZIP codes. The F_1 scores of LSPC and PCD are 0.41 and 0.57, respectively, and the Hamming distances of LSPC and PCD are 162 and 141, respectively.

the selected ZIP code; and the noise $\epsilon \sim \mathcal{N}(0, \sigma^2 \mathbf{I})$ with σ^2 varying from 0.1 to 1 with interval 0.1. At each noise level, we generate 1,000 piecewise-constant graph signals. Figure 9(a) shows a piecewise-constant signal generated by ZIP codes 10022 and 10030 and (b) shows a noisy graph signal with noise variance $\sigma^2 = 1$. We use the local-set-based piecewise-constant dictionary (LSPC) [15] and piecewise-constant decomposition (13) (PCD) to decompose this noisy graph signal into two activated pieces. We did not compare with hard thresholding, trend filtering and graph Laplacian denoising because it is difficult to determine thresholds for multiple pieces with various activated magnitudes. Figures 9(c)–(d) show the results provided by LSPC and PCD, respectively. We see that LSPC fails to localize ZIP code 10030, but PCD successfully localizes both ZIP codes and provides acceptable localization performance.

To quantify the localization performance, we again use the F_1 score and the Hamming distance. Figures (10)(a)–(b) show the F_1 score and Hamming distance when localizing ZIP codes in Manhattan as a function of noise level. The results at each noise level are averaged over 1,000 runs. Again, we see that PCD provides significantly better performance than LSPC, but PCD is sensitive to noise, while LSPC is robust to noise.

2) *Restaurant and taxi-pickups:* We now analyze restaurant density and taxi-pickup activity in Manhattan with the aim of understanding their components through decomposition.

Figure 12(a) shows the restaurant density including the positions of 10,121 restaurants in Manhattan. We project each restaurant to its nearest intersection and count the number of restaurants at each intersection. We use piecewise-constant decomposition to decompose this graph signal. Figures 12(c)–(d) show the decomposition by using three and nine pieces,

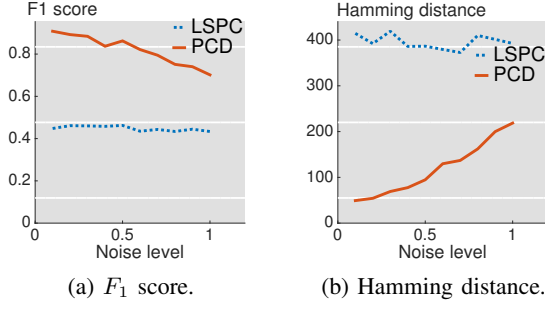


Fig. 10: Localizing multiple ZIP codes as a function of noise level. The proposed PCD significantly outperforms LSPC.

respectively. Through the decomposition, we can get a rough idea about the distribution of restaurants. For example, areas around East Village and Times Square have more restaurants. By using more pieces, we can obtain a finer resolution and a better approximation.

Figure 12(b) shows the approximation error where the x -axis is the number of expansion coefficients and the y -axis is the normalized mean-squared error. We compare nonlinear approximation by using graph Fourier basis based on the adjacency matrix [1] (graph Fourier (A), yellow-square line), nonlinear approximation by using graph Fourier basis based on the graph Laplacian matrix [3] (graph Fourier (L), purple-square line), sparse coding based on vertex-frequency based graph dictionary [47] (v-f gDictionary, blue-dashed line), egonet based localized patterns suggested in [13] (20-hop patterns, green-dashed line), local-set-based piecewise-constant graph dictionary [15] (LSPC, blue-solid line) and piecewise-constant decomposition (13) (PCD, red-solid line). The vertex-frequency based graph dictionary, or windowed graph Fourier transform, is a graph-frequency domain based representation, which produces the graph spectrogram and enables vertex-frequency analysis. In the experiments, we use four graph filters for vertex-frequency based graph dictionary, which includes 54,716 atoms in total. [13] suggests a graph dictionary where each atom activates a K -hop neighbor. In the experiments, we put all neighbors up to 20 hops into a graph dictionary, which includes 273,580 atoms. Note that the local-set-based piecewise-constant graph dictionary includes 27,357 atoms and the proposed piecewise-constant decomposition adaptively learns a small number of atoms (equal to the number of coefficients) from the given graph signal.

Figure 12(d) shows that by using the same number of expansion coefficients (pieces), piecewise-constant decomposition significantly outperforms other methods; egonet-based localized patterns also provide good results but are not flexible enough to capture localized patterns with arbitrary shapes; the vertex-frequency based graph dictionary fails because as it does not capture localized variations as well as the vertex-domain based representations; and graph Fourier basis based on adjacency matrix [1] outperforms the one based on the Laplacian matrix [3]. Overall, piecewise-constant decomposition provides an effective data-adaptive and structure-related representation.

Figure 13(a) shows the Manhattan taxi-pickup activity on Friday, June 5th, at 11 pm. We project each taxi pickup to its nearest intersection, count the number of pickups and

use piecewise-constant decomposition to decompose this graph signal. Figures 13(c)–(d) show the decomposition with three and nine pieces, respectively. This decomposition allows us to get a rough idea of the taxi pickup distribution; for example, areas around East Village and Times Square are busier.

Figure 13(b) shows the approximation error. Similarly to the results for the restaurant distribution, we see that using the same number of expansion coefficients (pieces), piecewise-constant decomposition significantly outperforms the other methods and graph Fourier basis based on the adjacency matrix [1] outperforms the one based on the graph Laplacian matrix [3].

Note that both the restaurant distribution and the taxi-pickup activity on Friday nights activate the areas around East Village and Times Square (see Figure 14). Each piece in Figure 14 comes from one of the three pieces in Figures 12(c) and 13(c); we observe that the corresponding pieces highly overlap. The F_1 score between the two *Times Square* pieces is 0.65 and the F_1 score between the two *East Village* pieces is 0.59 indicating that the taxi pickups on Friday nights are highly correlated with the restaurant distribution, confirming a well-understood pattern of urban lifestyle.

IV. DICTIONARY LEARNING ON GRAPHS

We now extend signal decomposition, where we find activated pieces from a single graph signal, to dictionary learning where the aim is to find activated pieces shared by multiple graph signals. In other words, we learn activated pieces as building blocks that are used to represent multiple graph signals. We extend the decomposition solver from Section III to the dictionary learning problem and apply it to mine traffic patterns in the Manhattan data set.

Consider a matrix of L graph signals as columns,

$$X = DZ + E \in \mathbb{R}^{N \times L},$$

with $D = [\mathbf{1}_{C_1} \ \mathbf{1}_{C_2} \ \cdots \ \mathbf{1}_{C_K}]$ the graph dictionary with a predefined number of K one-piece atoms as columns, the coefficient matrix $Z \in \mathbb{R}^{K \times L}$ is sparse, C_i are connected and $E_{i,j} \sim \mathcal{N}(0, \sigma^2)$ is Gaussian noise. We store activated pieces in D as building blocks. Thus, each graph signal (column in X) is approximated by a linear combination of several pieces from D . We learn the pieces C_i from X by solving

$$\begin{aligned} \min_{Z, C_i} & \|X - [\mathbf{1}_{C_1} \ \mathbf{1}_{C_2} \ \cdots \ \mathbf{1}_{C_K}] Z\|_2^2, \\ \text{subject to } & C_i \in \mathcal{C} \quad \text{and} \quad \|Z\|_{0,\infty} \leq S, \end{aligned} \quad (14)$$

where the sparsity level S helps avoid overfitting and $\|Z\|_{0,\infty} = \max_{i=1,\dots,N} \|\mathbf{z}_i\|_0$ with \mathbf{z}_i the i th column in Z , which is the maximum number of nonzero elements in each column. When the number of graph signals $L = 1$, the dictionary learning problem becomes the decomposition problem (13).

Note that this graph dictionary is not designed to learn from arbitrary graph signals. Due to the strong connectivity constraints, (14) is not flexible enough to approximate a graph signal as well as using the classical K-SVD; the advantage, however, is that it can find shared localized patterns from a large set of graph signals, which K-SVD cannot do as it would require careful threshold tuning for each selected atom.

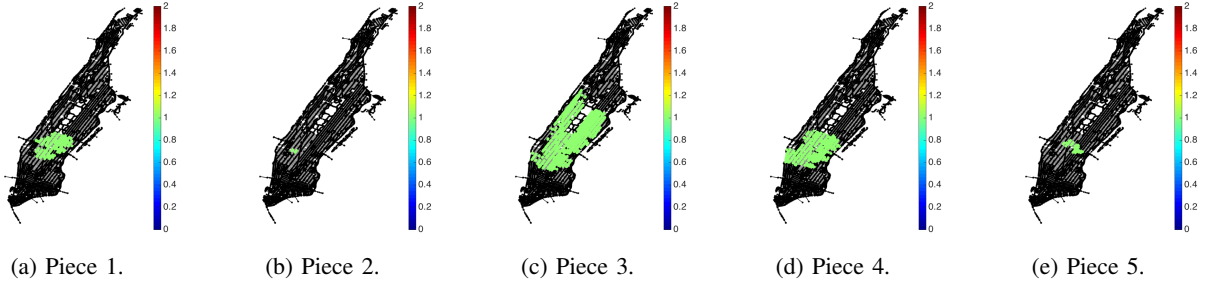


Fig. 11: Top five most frequently-used pieces learned from taxi-pickup activities during rush hours in 2015.

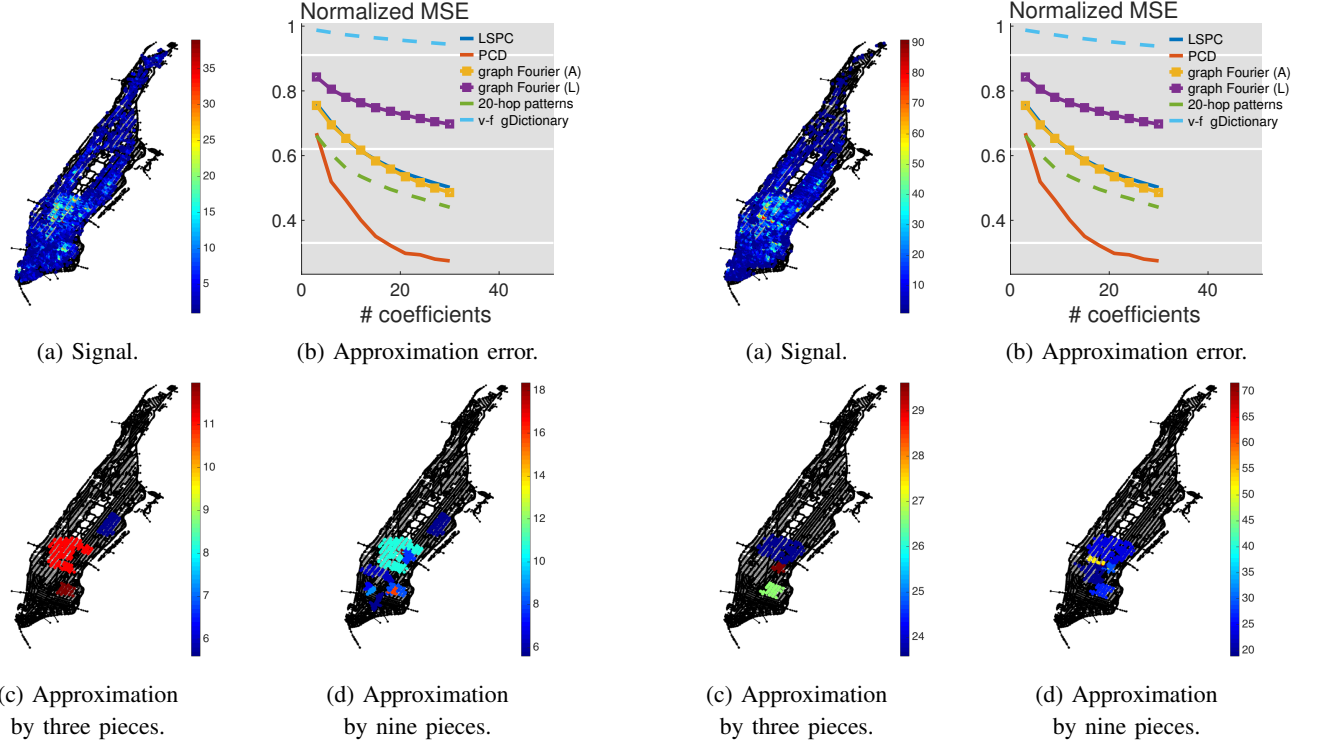


Fig. 12: Decomposing the restaurant distribution in Manhattan using a piecewise-constant decomposition. Piecewise-constant decomposition (PCD) (13) outperforms the other methods in the task of approximation.

A. Methodology

Our goal is to learn shared pieces and the corresponding coefficients from a matrix of graph signals. While it would also be possible to use the decomposition techniques from the previous section to localize pieces from each graph signal and store all activated pieces into the dictionary, that approach would not reveal correlations among graph signals. We use the learning approach to find shared pieces among several graph signals as it allows the same piece to be repeatedly used as a basic building block thus revealing correlations.

To solve (14), we update the dictionary and the coefficient matrix successively; that is, given the dictionary, we optimize over the coefficient matrix and then, given the coefficient matrix, we optimize over the dictionary. When updating the

Fig. 13: Decomposing the taxi-pickup activity in Manhattan On Friday, June 5th, at 11 pm, using a piecewise-constant decomposition. Piecewise-constant decomposition (PCD) (13) outperforms the other methods in the task of approximation.

coefficient matrix, we fix C_i and consider

$$\min_Z \|X - [\mathbf{1}_{C_1} \ \mathbf{1}_{C_2} \ \cdots \ \mathbf{1}_{C_K}] Z\|_F^2, \quad (15)$$

subject to $\|Z\|_{0,\infty} \leq S$.

where $\|\cdot\|_F$ denotes the Frobenius norm. This is a common sparse coding problem, which can be efficiently solved by orthogonal matching pursuit [63]. When updating the graph dictionary, we fix Z and consider

$$\min_{C_i} \|X - [\mathbf{1}_{C_1} \ \mathbf{1}_{C_2} \ \cdots \ \mathbf{1}_{C_K}] Z\|_F^2, \quad (16)$$

subject to $C_i \in \mathcal{C}$.

Similarly to the piecewise-constant decomposition, we iteratively update each piece. Let \mathbf{z}_i be the i th row of Z and

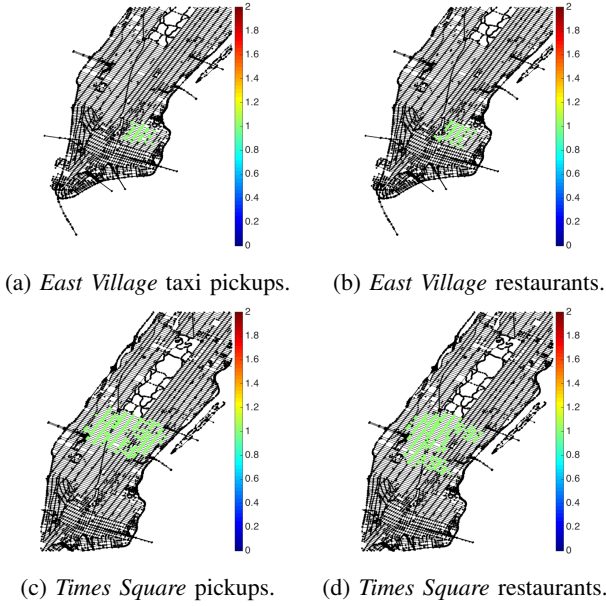


Fig. 14: Both restaurant distribution and taxi-pickup activity on Friday nights activate the same areas around East Village and Times Square. The F_1 score between the two *Times Square* pieces is 0.65 and the F_1 score between the two *East Village* pieces is 0.59, indicating a high overlap.

$R_j = X - \sum_{i \neq j} \mathbf{1}_{C_i} \mathbf{z}_i^T \in \mathbb{R}^{N \times L}$. Then,

$$\begin{aligned} & \|X - [\mathbf{1}_{C_1} \quad \mathbf{1}_{C_2} \quad \cdots \quad \mathbf{1}_{C_K}] Z\|_F^2 \stackrel{(a)}{=} \|R_j - \mathbf{1}_{C_j} \mathbf{z}_j^T\|_F^2 \\ & \stackrel{(b)}{=} \text{Tr}(R_j^T R_j - R_j^T \mathbf{1}_{C_j} \mathbf{z}_j^T - \mathbf{z}_j \mathbf{1}_{C_j}^T R_j + \mathbf{z}_j \mathbf{1}_{C_j}^T \mathbf{1}_{C_j} \mathbf{z}_j^T) \\ & \stackrel{(c)}{=} \text{Tr}(R_j^T R_j) + (\mathbf{z}_j^T \mathbf{z}_j \mathbf{1} - 2 R_j \mathbf{z}_j)^T \mathbf{1}_{C_j}, \end{aligned}$$

where (a) follows from the denotation of R_j , (b) from the definition of Frobenius norm and the trace operator, and (c) from $\text{Tr}(XY) = \text{Tr}(YX)$. Since the first term is a constant, to update each piece, we freeze all the other pieces and solve

$$\min_{C_i} (\mathbf{z}_j^T \mathbf{z}_j \mathbf{1} - 2 R_j \mathbf{z}_j)^T \mathbf{1}_{C_i}, \quad \text{subject to } C_i \in \mathcal{C},$$

where the objective function is an inner product of two vectors. This is equivalent to solving the localization problem (4) by setting $\mathbf{x} = R_j \mathbf{z}_j / \mathbf{z}_j^T \mathbf{z}_j$; that is,

$$\begin{aligned} & \left\| \frac{R_j \mathbf{z}_j}{\mathbf{z}_j^T \mathbf{z}_j} - \mathbf{1}_{C_i} \right\|_2^2 = \frac{1}{(\mathbf{z}_j^T \mathbf{z}_j)^2} \|R_j \mathbf{z}_j - \mathbf{z}_j^T \mathbf{z}_j \mathbf{1}_{C_i}\|_2^2 \\ & = \frac{\mathbf{z}_j^T R_j^T R_j \mathbf{z}_j}{(\mathbf{z}_j^T \mathbf{z}_j)^2} + \frac{1}{\mathbf{z}_j^T \mathbf{z}_j} (\mathbf{z}_j^T \mathbf{z}_j \mathbf{1}_{C_i}^T \mathbf{1}_{C_i} - 2(R_j \mathbf{z}_j)^T \mathbf{1}_{C_i}), \end{aligned}$$

where $\mathbf{z}_j^T \mathbf{z}_j$ is a scalar and $\mathbf{1}_{C_i}^T \mathbf{1}_{C_i} = \mathbf{1}^T \mathbf{1}_{C_i}$ because $\mathbf{1}_{C_i}$ is a binary vector. In other words, we update each piece in the graph dictionary by using the localization solver (11). We iteratively update each piece until convergence and we obtain a series of solutions providing a local optimum [62].

B. Experimental Validation

We use the dictionary learning techniques (15)–(16) to mine taxi-pickup patterns in Manhattan, as taxis are valuable sensors

of city life [64], [65], [66], providing insight into economic activity, human behavior and mobility patterns. We consider the 2015 public dataset of taxi pickups (used in Section III-B) during rush hour (6-8pm). We add taxi pickups within each hour to obtain 1,095 (365×3) graph signals; thus, each graph signal is a measure of taxi pickups at an intersection in Manhattan at a specific hour. We mine pickup patterns through two tasks: detecting events in Manhattan and checking whether weekdays and weekends exhibit differences in traffic patterns.

1) *Dictionary Learning on Graphs: Event detection:* We consider two types of events: common events and special events. A common event usually leads to a place that is frequently or periodically crowded, which shows a natural traffic behavior, and a special event usually leads to a place that is rarely crowded, which shows an anomaly in traffic behavior. Traffic accidents or holiday celebrations usually lead to special events. We are going to use the learned pieces and their corresponding coefficients to analyze the taxi-pickup activities during rush hours. We set the size of the dictionary to $K = 500$ and its sparsity to $S = 30$. This means that $K = 500$ activated pieces are learned from $L = 1,095$ graph signals of dimension $N = 13,679$ (13,679 intersections in Manhattan) and each graph signal is approximated by at most 30 pieces. When a piece is used to represent a graph signal, it means that the corresponding area is particularly crowded at a specific time and we need this piece to capture this traffic information. On the other hand, when a piece is not used, it just means that the corresponding area is not particularly crowded compared to other areas; it does not necessarily mean that there are no taxi pickups in the corresponding area because those taxi pickups may activate other related pieces.

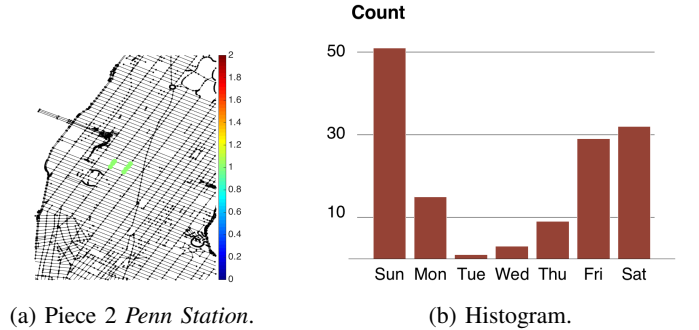


Fig. 15: When is Penn Station particularly crowded compared to other places? (a) Precise locations of Piece 2. (b) Histogram indicating that Penn Station is significantly more crowded than other places during weekends.

Common events. Common events show natural traffic behaviors, which are detected by frequently-used pieces. When a row in the coefficient matrix has many nonzero entries, the corresponding piece is frequently used to represent graph signals. The top five most frequently-used pieces learned from taxi-pickup activities during rush hours are shown in Figure 11. For example, Figure 11(b) shows that a small area around Penn Station is frequently crowded and we use Piece 2 to capture this information. We then check which day uses this piece. Figure 15(b) shows a histogram of the usage, where we see

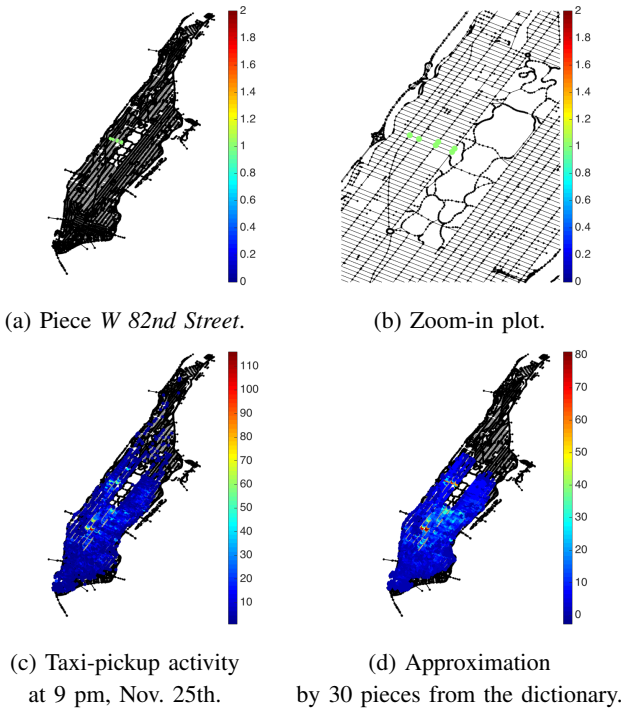


Fig. 16: Inflation of the balloons the day before Macy's Thanksgiving Parade is detected. 6-8 pm on Nov 25th activates the 466th piece, indicating locations around W 82nd Street are particularly crowded.

that Piece 2 is more frequently used on Sundays (as well as Fridays and Saturdays) during the entire 2015. This indicates that, compared to other places in Manhattan, Penn Station is particularly crowded during weekends. This is intuitive due to a large number of commuters going through Penn Station and visiting the nearby Madison Square Garden on weekends.

Special events. Special events show anomalous traffic behaviors, which are detected by the rarely-used pieces. When a row in the coefficient matrix has a few nonzero entries, the corresponding piece is rarely used to represent graph signals. Figure 16(a) shows the 466th piece in the graph dictionary activating the area around West 82nd street and (b) shows a zoom-in plot. This piece is only used three times during the entire year of 2015, between 6-8 pm on November 25th, the night before Thanksgiving Day, indicating that the area around West 82nd street was much more crowded compared to other areas on that night only. Figures 16(c)–(d) show the taxi-pickup activities at 9 pm on November 25th and its approximation by using the graph dictionary, respectively. This event actually corresponds to the inflation of the balloons for the Macy's Thanksgiving parade that happens on 77th and 81st streets between Columbus and Central Park West, purely from the taxi-pickup activity.

Figure 17(a) shows the 377th piece in the graph dictionary activating the area around Apple Store on 5th Avenue and (b) shows a zoom-in plot. This piece is only used one time during the entire year of 2015, that is, 8 pm on July 3rd, the night before Independence Day. This indicates that the area around Apple Store on 5th Avenue was much more crowded compared

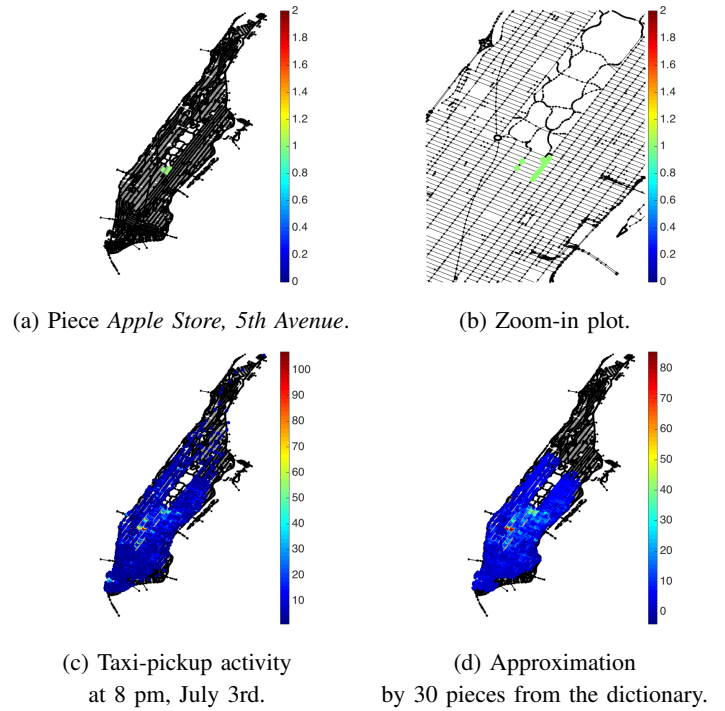


Fig. 17: 8 pm on July 3rd activates the 377th piece, indicating that the 5th Ave. Apple store area is particularly crowded.

to other areas on that night only. Figures 17(c)–(d) show the taxi-pickup activities at 8 pm on July 3rd and its approximation by using the graph dictionary, respectively.

2) *What day is today in Manhattan?*: Are traffic patterns on weekends different from traffic patterns on weekdays? We use the learned graph dictionary to answer this question.

Graph dictionary learning not only provides traffic-correlated pieces, but also extracts traffic-correlated features through approximation. Similarly to principal component analysis, graph-dictionary-based sparse representation corresponds to unsupervised learning; it reduces the dimension of the representation, thereby extracting key information. Unlike principal component analysis, which is unaware of the graph structure, graph-dictionary-based sparse representation extracts traffic-correlated features based on the graph structure. Since there are 500 pieces in the graph dictionary, we reduce the dimension of each graph signal from 13,679 to 500 and the corresponding 500 expansion coefficients are traffic-correlated features.

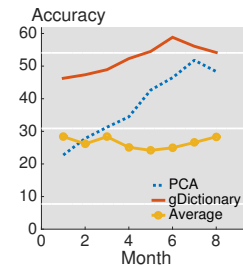


Fig. 18: Classifying to which day a graph signal belongs. Graph-dictionary-based sparse representation significantly outperforms principal component analysis.

We now consider a seven-class classification task: given a

graph signal, we aim to identify to which day of the week it belongs by using traffic-correlated features. Figure 18 shows the classification accuracy as a function of training data, where the x -axis is the number of months used in training and the y -axis is the classification accuracy. For example, when the month is $x = 1$, we use 93 (31×3) graph signals in January as training data and use the remaining 1002 graph signals as testing data. Since this task involves seven classes, classification accuracy of a random guess is 14.29%. We compare three methods: principal component analysis with top 500 components (PCA, blue dotted line), average value of each graph signal (Average, yellow-circle line) and the graph-dictionary-based sparse representation (gDictionary, red solid line). We see that graph-dictionary-based sparse representation significantly outperforms principal component analysis and the average value. The classification accuracy of graph-dictionary-based sparse representation increases as the number of training data grows before July after which it drops slightly, showing that summer traffic patterns are distinctive.

We now fix January graph signals as training data and the graph signals in the remaining 11 months as testing data; Figure 19(a) shows the classification confusion matrix.⁴ It is relatively easy to distinguish weekdays from weekends as well as Saturdays from Sundays; in contrast, weekdays are easily confused with each other indicating similar traffic patterns.

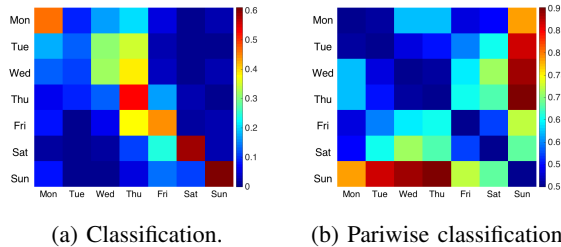


Fig. 19: (a) Classification and (b) pairwise confusion matrices using January graph signals as training data showing that it is relatively easy to distinguish weekdays from weekends.

We then run a series of pairwise classifications to see whether traffic patterns on weekdays and weekends differ. We only consider distinguishing one weekday from another at a time. Figure 19(b) shows pairwise classification accuracies; we can easily distinguish Sundays from weekdays, but not weekdays from other weekdays.

3) *Discussion:* We detected events and classified days of the week from taxi pickups in Manhattan. We were able to successfully detect locations and times of both common and special events by using the graph dictionary learned from a spatio-temporal taxi-pickup data volume. In day-of-the-week classification, we were able to significantly outperform principal component analysis and provide insight into the traffic patterns on weekdays and weekends by using the same graph dictionary. These results suggest that the proposed graph dictionary learning techniques are a promising tool for exploring mobility patterns of spatio-temporal urban data, which may aid in urban planning and traffic forecasting.

⁴Given c classes and confusion matrix $M \in \mathbb{R}^{c \times c}$, element $M_{i,j}$ is a count of samples that belong to class i but are classified as class j . Perfect classification yields an identity confusion matrix.

V. CONCLUSIONS

We studied three critical problems allowing piecewise-constant graph signals to serve as a tool for mining large amounts of complex data: graph signal localization, graph signal decomposition and graph dictionary learning. We used piecewise-constant graph signals to model local information in the vertex-domain and showed that decomposition and dictionary learning are natural extensions of localization. For each of these three problems, we proposed a specific graph signal model, an optimization problem and an efficient solver.

We conducted extensive validation studies on diverse datasets. The results show that cut-based localization is good at localizing ball-shaped classes and path-based localization is good at localizing elongated class. We also used proposed methods to analyze taxi-pickup activity in Manhattan in 2015 and showed that based on these, we can successfully detect both common and special events as well as tell apart weekdays from weekends. These findings validate the effectiveness of the proposed methods and suggest that graph signal processing tools may aid in urban planning and traffic forecasting.

REFERENCES

- [1] A. Sandryhaila and J. M. F. Moura, "Discrete signal processing on graphs," *IEEE Trans. Signal Process.*, vol. 61, no. 7, pp. 1644–1656, Apr. 2013.
- [2] A. Sandryhaila and J. M. F. Moura, "Big data processing with signal processing on graphs," *IEEE Signal Process. Mag.*, vol. 31, no. 5, pp. 80–90, Sept. 2014.
- [3] D. I. Shuman, S. K. Narang, P. Frossard, A. Ortega, and P. Vandergheynst, "The emerging field of signal processing on graphs: Extending high-dimensional data analysis to networks and other irregular domains," *IEEE Signal Process. Mag.*, vol. 30, pp. 83–98, May 2013.
- [4] A. Anis, A. Gadde, and A. Ortega, "Efficient sampling set selection for bandlimited graph signals using graph spectral proxies," *IEEE Trans. Signal Process.*, vol. 64, no. 14, pp. 3775–3789, 2015.
- [5] S. Chen, R. Varma, A. Sandryhaila, and J. Kovačević, "Discrete signal processing on graphs: Sampling theory," *IEEE Trans. Signal Process.*, vol. 63, no. 24, pp. 6510–6523, Dec. 2015.
- [6] A. G. Marques, S. Segarra, G. Leus, and A. Ribeiro, "Sampling of graph signals with successive local aggregations," *IEEE Trans. Signal Process.*, vol. 64, pp. 1832–1843, Dec. 2015.
- [7] S. Chen, R. Varma, A. Singh, and J. Kovačević, "Signal recovery on graphs: Fundamental limits of sampling strategies," *IEEE Trans. Signal and Inform. Process. over Networks*, 2016, Submitted.
- [8] S. Chen, A. Sandryhaila, J. M. F. Moura, and J. Kovačević, "Signal recovery on graphs: Variation minimization," *IEEE Trans. Signal Process.*, vol. 63, no. 17, pp. 4609–4624, Sept. 2015.
- [9] S. Chen, F. Cerda, P. Rizzo, J. Bielak, J. H. Garrett, and J. Kovačević, "Semi-supervised multiresolution classification using adaptive graph filtering with application to indirect bridge structural health monitoring," *IEEE Trans. Signal Process.*, vol. 62, no. 11, pp. 2879–2893, June 2014.
- [10] S. K. Narang, Akshay Gadde, and Antonio Ortega, "Signal processing techniques for interpolation in graph structured data," in *Proc. IEEE Int. Conf. Acoust., Speech, Signal Process.*, Vancouver, May 2013, pp. 5445–5449.
- [11] M. S. Kotzagiannidis and P. L. Dragotti, "Sampling and reconstruction of sparse signals on circulant graphs—an introduction to graph-fri," *arXiv preprint arXiv:1606.08085*, 2016.
- [12] X. Zhu and M. Rabbat, "Approximating signals supported on graphs," in *Proc. IEEE Int. Conf. Acoust., Speech, Signal Process.*, Kyoto, Mar. 2012, pp. 3921–3924.
- [13] D. Thanou, D. I. Shuman, and P. Frossard, "Learning parametric dictionaries for signals on graphs," *IEEE Trans. Signal Process.*, vol. 62, pp. 3849–3862, June 2014.
- [14] N. Tremblay and P. Borgnat, "Subgraph-based filterbanks for graph signals," *IEEE Trans. Signal Process.*, vol. 64, pp. 3827–3840, Mar. 2016.
- [15] S. Chen, T. Ji, R. Varma, A. Singh, and J. Kovačević, "Signal representations on graphs: Tools and applications," *IEEE Trans. Signal Process.*, Mar. 2016, Submitted.

- [16] A. Agaskar and Y. M. Lu, "A spectral graph uncertainty principle," *IEEE Trans. Inf. Theory*, vol. 59, no. 7, pp. 4338–4356, July 2013.
- [17] M. Tsitsvero, S. Barbarossa, and P. D. Lorenzo, "Signals on graphs: Uncertainty principle and sampling," *arXiv:1507.08822*, 2015.
- [18] N. Perraudin and P. Vandergheynst, "Stationary signal processing on graphs," *arXiv preprint arXiv:1603.04667*, Jan. 2016.
- [19] A. G. Marques, S. Segarra, G. Leus, and A. Ribeiro, "Stationary graph processes and spectral estimation," *arXiv preprint arXiv:1603.04667*, Mar. 2016.
- [20] S. K. Narang and A. Ortega, "Perfect reconstruction two-channel wavelet filter banks for graph structured data," *IEEE Trans. Signal Process.*, vol. 60, pp. 2786–2799, June 2012.
- [21] S. K. Narang and A. Ortega, "Compact support biorthogonal wavelet filterbanks for arbitrary undirected graphs," *IEEE Trans. Signal Process.*, vol. 61, no. 19, pp. 4673–4685, Oct. 2013.
- [22] V. N. Ekambaram, G. C. Fanti, B. Ayazifar, and K. Ramchandran, "Spline-like wavelet filterbanks for multiresolution analysis of graph-structured data," *IEEE Trans. Signal and Information Processing over Networks*, vol. 1, no. 4, pp. 268–278, 2015.
- [23] J. Zeng, G. Cheung, and A. Ortega, "Bipartite subgraph decomposition for critically sampled wavelet filterbanks on arbitrary graphs," in *Proc. IEEE Int. Conf. Acoust., Speech, Signal Process.*, Shanghai, Mar. 2016, pp. 6210–6214.
- [24] S. Chen, A. Sandryhaila, J. M. F. Moura, and J. Kovačević, "Signal denoising on graphs via graph filtering," in *Proc. IEEE Glob. Conf. Signal Information Process.*, Atlanta, GA, Dec. 2014, pp. 872–876.
- [25] N. Tremblay and P. Borgnat, "Graph wavelets for multiscale community mining," *IEEE Trans. Signal Process.*, vol. 62, pp. 5227–5239, Oct. 2014.
- [26] X. Dong, P. Frossard, P. Vandergheynst, and N. Nefedov, "Clustering on multi-layer graphs via subspace analysis on Grassmann manifolds," *IEEE Trans. Signal Process.*, vol. 62, no. 4, pp. 905–918, Feb. 2014.
- [27] P.-Y. Chen and A.O. Hero, "Local Fiedler vector centrality for detection of deep and overlapping communities in networks," in *Proc. IEEE Int. Conf. Acoust., Speech, Signal Process.*, Florence, 2014, pp. 1120–1124.
- [28] D. K. Hammond, P. Vandergheynst, and R. Gribonval, "Wavelets on graphs via spectral graph theory," *Appl. Comput. Harmon. Anal.*, vol. 30, pp. 129–150, Mar. 2011.
- [29] S. I. K. Narang, G. Shen, and A. Ortega, "Unidirectional graph-based wavelet transforms for efficient data gathering in sensor networks," in *Proc. IEEE Int. Conf. Acoust., Speech, Signal Process.*, Dallas, TX, Mar. 2010, pp. 2902–2905.
- [30] D. I. Shuman, M. J. Faraji, and P. Vandergheynst, "A multiscale pyramid transform for graph signals," *IEEE Trans. Signal Process.*, vol. 64, pp. 2119–2134, Apr. 2016.
- [31] S. Zhang and M. A. Karim, "A new impulse detector for switching median filters," *IEEE Signal Process. Lett.*, vol. 9, no. 12, pp. 360–363, Nov. 2002.
- [32] J. D. Haupt, R. M. Castro, and R. D. Nowak, "Distilled sensing: selective sampling for sparse signal recovery," in *Proceedings of the Twelfth International Conference on Artificial Intelligence and Statistics, AISTATS*, Clearwater Beach, Florida, April 2009, pp. 216–223.
- [33] K. Kim, T. H. Chalidabhongse, D. Harwood, and L. Davis, "Real-time foreground-background segmentation using codebook model," *Real-Time Imaging*, vol. 11, no. 3, pp. 172–185, June 2005.
- [34] F. Buggenthin, C. Marr, M. Schwarzfischer, P. S. Hoppe, O. Hilsenbeck, T. Schroeder, and F. J. Theis, "An automatic method for robust and fast cell detection in bright field images from high-throughput microscopy," *BMC Bioinformatics*, vol. 14, pp. 297, 2013.
- [35] G. L. Turin, "An introduction to matched filters," *IRE Trans. Information Theory*, vol. 6, no. 3, pp. 311–329, 1960.
- [36] D. O. North, "An analysis of the factors which determine signal/noise discrimination in pulsed-carrier systems," *Proceedings of the IEEE*, vol. 51, pp. 10161027, July 1963.
- [37] R. C. Gonzalez and R. E. Woods, *Digital Image Processing*, Prentice Hall, Englewood Cliffs, NJ, 2002.
- [38] C. Faloutsos, "Large graph mining: patterns, cascades, fraud detection, and algorithms," in *Proc. Int. World Wide Web Conf.*, 2014, pp. 1–2.
- [39] E. Arias-Castro, E. J. Candès, and A. Durand, "Detection of an anomalous cluster in a network," *Ann. Stat.*, vol. 39, no. 1, pp. 278–304, 2011.
- [40] C. Hu, L. Cheng, J. Sepulcre, G. E. Fakhri, Y. M. Lu, and Q. Li, "Matched signal detection on graphs: Theory and application to brain network classification," in *Proc. Int. Conf. Inf. Process. Med. Imaging*, Pacific Grove, CA, 2013.
- [41] J. Sharpnack, A. Krishnamurthy, and A. Singh, "Detecting activations over graphs using spanning tree wavelet bases," in *AISTATS*, Scottsdale, AZ, Apr. 2013.
- [42] J. Sharpnack, A. Krishnamurthy, and A. Singh, "Near-optimal anomaly detection in graphs using Lovasz extended scan statistic," in *Proc. Neural Information Process. Syst.*, 2013.
- [43] S. Chen, Y. Yang, S. Zong, A. Singh, and J. Kovačević, "Detecting structure-correlated attributes on graphs," *IEEE Trans. Signal Process.*, 2016, Submitted.
- [44] M. Vetterli, J. Kovačević, and V. K. Goyal, *Foundations of Signal Processing*, Cambridge University Press, Cambridge, 2014, <http://foundationsofsignalprocessing.org>.
- [45] J. Kovačević, V. K. Goyal, and M. Vetterli, *Fourier and Wavelet Signal Processing*, Cambridge University Press, Cambridge, 2016, <http://www.fourierandwavelets.org/>.
- [46] C. M. Bishop, *Pattern Recognition and Machine Learning*, Information Science and Statistics. Springer, 2006.
- [47] D. I. Shuman, B. Ricaud, and P. Vandergheynst, "Vertex-frequency analysis on graphs," *Appl. Comput. Harmon. Anal.*, vol. 40, pp. 260–291, March 2016.
- [48] R. R. Coifman and M. Maggioni, "Diffusion wavelets," *Appl. Comput. Harmon. Anal.*, pp. 53–94, July 2006.
- [49] M. Gavish, B. Nadler, and R. R. Coifman, "Multiscale wavelets on trees, graphs and high dimensional data: Theory and applications to semi supervised learning," in *Proc. Int. Conf. Mach. Learn.*, Haifa, Israel, June 2010, pp. 367–374.
- [50] M. Crovella and E. Kolaczyk, "Graph wavelets for spatial traffic analysis," in *Proc. IEEE INFOCOM*, Mar. 2003, vol. 3, pp. 1848–1857.
- [51] K. Engan, S. O. Aase, and J. H. Husøy, "Method of optimal directions for frame design," in *Proc. IEEE Int. Conf. Acoust., Speech, Signal Process.*, Phoenix, AZ, Mar. 1999, pp. 2443–2446.
- [52] M. Aharon, M. Elad, and A. Bruckstein, "K-SVD: An algorithm for designing overcomplete dictionaries for sparse representation," *IEEE Trans. Signal Process.*, vol. 54, no. 11, pp. 4311–4322, Nov. 2006.
- [53] J. Mairal, F. R. Bach, J. Ponce, and G. Sapiro, "Online dictionary learning for sparse coding," in *Proc. Int. Conf. Mach. Learn.*, Montreal, June 2009, pp. 689–696.
- [54] M. Newman, *Networks: An Introduction*, Oxford University Press, 2010.
- [55] Y. Boykov, O. Veksler, and R. Zabih, "Fast approximate energy minimization via graph cuts," *IEEE Trans. Pattern Anal. Mach. Intell.*, vol. 20, no. 11, pp. 1222–1239, Nov. 2001.
- [56] V. Kolmogorov and R. Zabih, "What energy functions can be minimized via graph cuts?," *IEEE Trans. Pattern Anal. Mach. Intell.*, vol. 26, no. 2, pp. 147–159, Feb. 2004.
- [57] T. H. Cormen, C. E. Leiserson, R. L. Rivest, and C. Stein, *Introduction to Algorithms*, MIT Press and McGrawHill, London, UK, 2 edition, 2001.
- [58] C. Chevalier and I. Safto, "Comparison of coarsening schemes for multilevel graph partitioning," in *Learning and Intelligent Optimization, Third International Conference*, Trento, Italy, Jan. 2009, pp. 191–205.
- [59] P. Liu, X. Wang, and Y. Gu, "Coarsening graph signal with spectral invariance," in *Proc. IEEE Int. Conf. Acoust., Speech, Signal Process.*, Florence, May 2014, pp. 1075–1079.
- [60] R. Duda, P. Hart, and D. Stork, *Pattern Classification*, John Wiley & Sons, Englewood Cliffs, NJ, 2001.
- [61] Y.-X. Wang, J. Sharpnack, A. Smola, and R. J. Tibshirani, "Trend filtering on graphs," in *AISTATS*, San Diego, CA, May 2015.
- [62] S. Boyd and L. Vandenberghe, *Convex Optimization*, Cambridge University Press, New York, NY, 2004.
- [63] Y. C. Pati, R. Rezaifar, and P. S. Krishnaprasad, "Orthogonal matching pursuit: Recursive function approximation with applications to wavelet decomposition," in *Proc. Asilomar Conf. Signal, Syst. Comput.*, Pacific Grove, CA, Nov. 1993, vol. 1, pp. 40–44.
- [64] N. Ferreira, J. Poco, H. T. Vo, J. Freire, and C. T. Silva, "Visual exploration of big spatio-temporal urban data: A study of New York City taxi trips," *IEEE Trans. Vis. Comput. Graphics*, vol. 19, no. 12, pp. 2149–2158, Dec. 2013.
- [65] H. Doraiswamy, N. Ferreira, T. Damoulas, J. Freire, and C. T. Silva, "Using topological analysis to support event-guided exploration in urban data," *IEEE Trans. Vis. Comput. Graphics*, vol. 20, no. 12, pp. 2634–2643, 2014.
- [66] J. A. Deri and J. M. F. Moura, "Taxi data in New York City: A network perspective," in *Proc. Asilomar Conf. Signal, Syst. Comput.*, Pacific Grove, CA, Nov. 2015, pp. 1829–1833.